Supporting Information

Confining Palladium Nanoparticles in Microporous Tetrastyrene Polymer Enables Efficient Size-Selective Heterogeneous Catalysis

Qiu Zhuang, Ruru Gao, Mingyang Shi, Xiangpeng Lin, Aming Xie,* and Wei Dong

1. Supported Figures

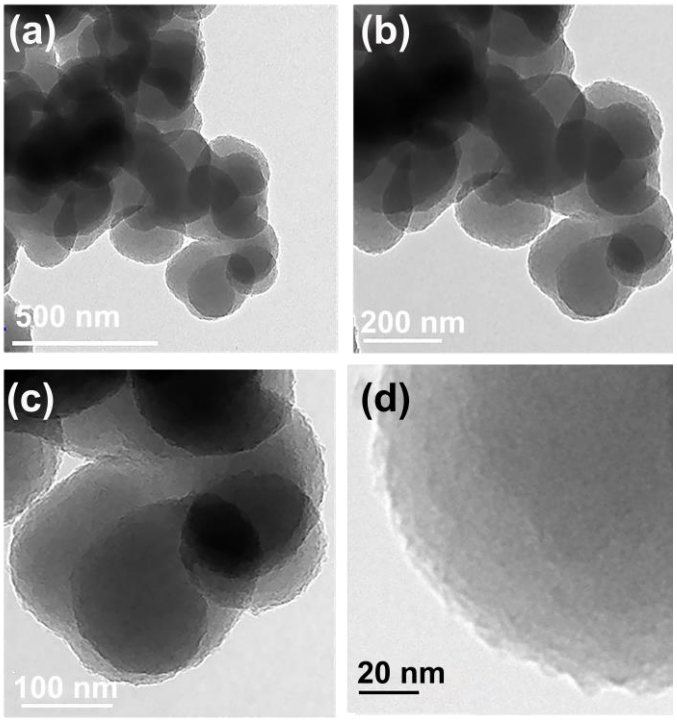

Figure S1. TEM images for Pd@MTP-1.

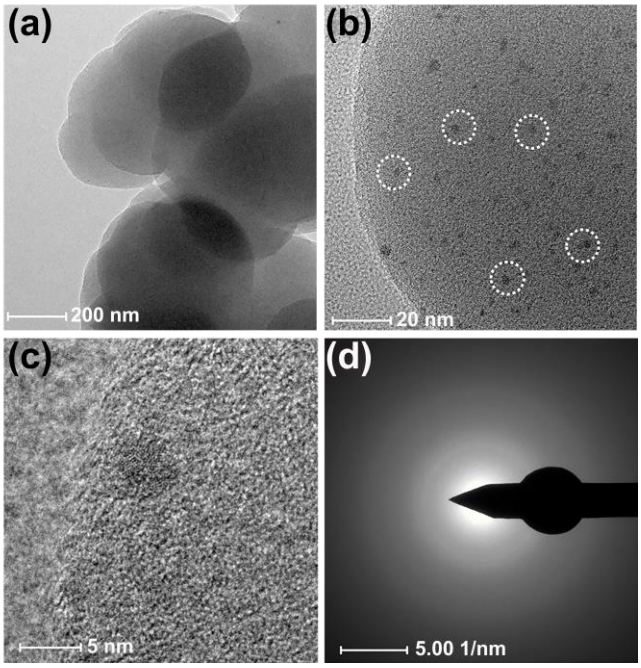

Figure S2. (a) TEM image, (b-c) HRTEM images, and (d) selected area electron diffraction (SAED) of Pd@MTP-2

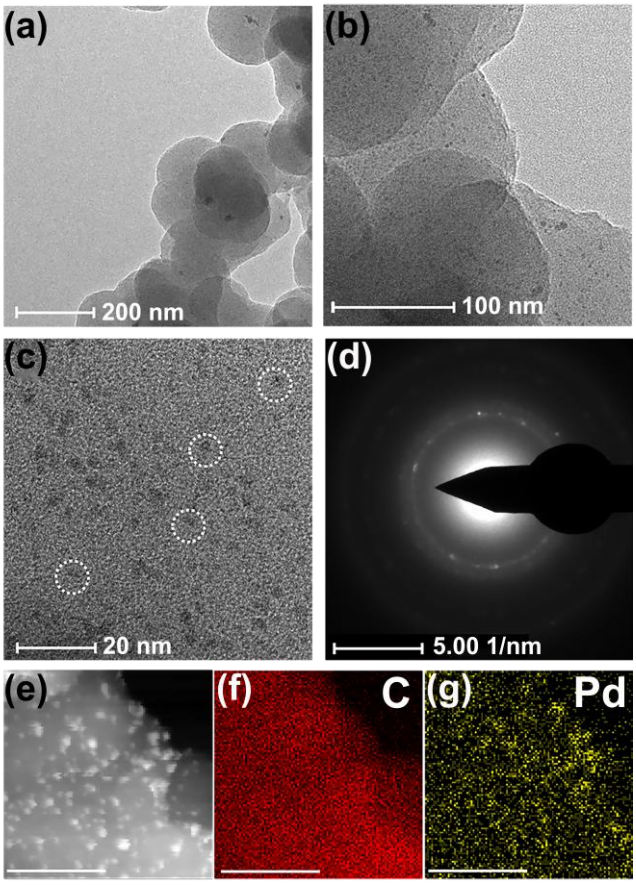

Figure S3. (a) TEM image, (b-c) HRTEM images, (d) selected area electron diffraction (SAED), and (e-f) scale bars are 100 nm, element mapping analysis of Pd@MTP-4.

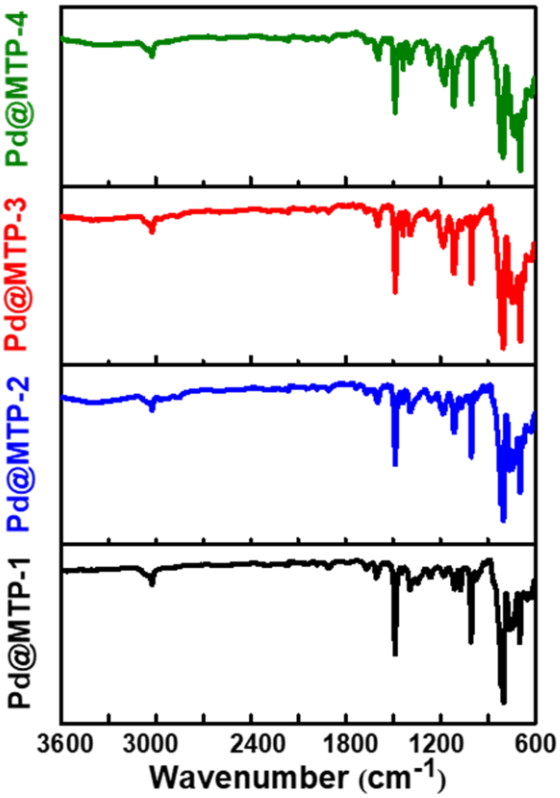

Figure S4. FT-IR spectra of Pd@MTP-1, Pd@MTP-2, Pd@MTP-3, and Pd@MTP-4.

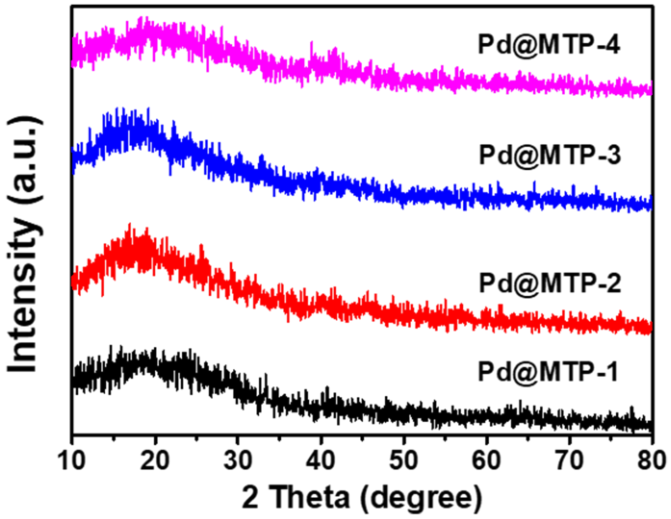

Figure S5. XRD spectra for Pd@MTP-1, Pd@MTP-2, Pd@MTP-3, and Pd@MTP-4.

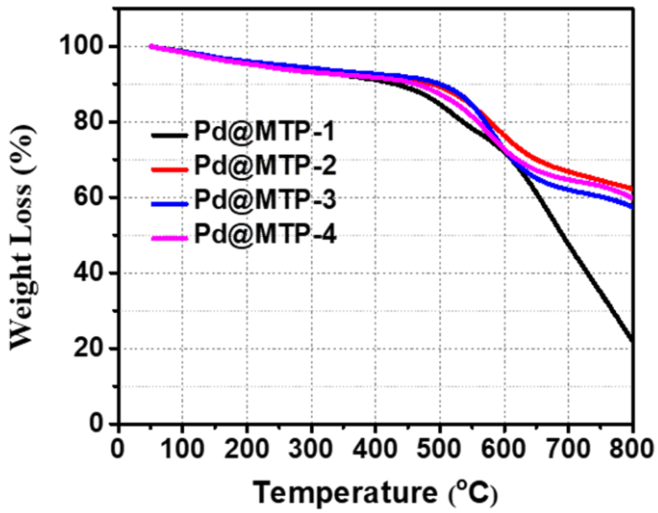

Figure S6. Thermogravimetric (TG) curves of Pd@MTP catalysts with a 10 °C/min heat rate at nitrogen atmosphere.

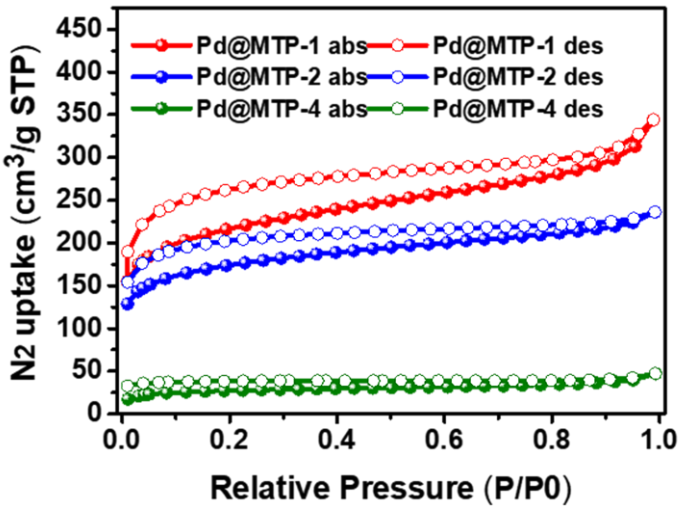

Figure S7. Nitrogen adsorption and desorption isotherm profiles of catalysts measured at 77.3 K.

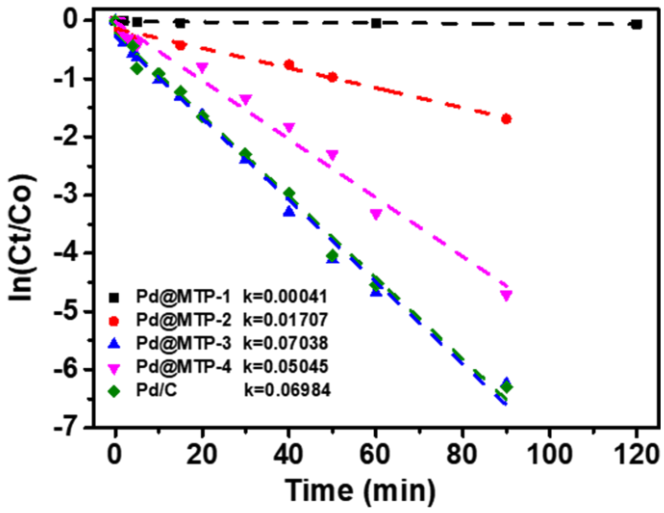

Figure S8. Relationship between $\ln(Ct/C_0)$ and the reaction time (t) for catalytic reduction of *p*-NPh.

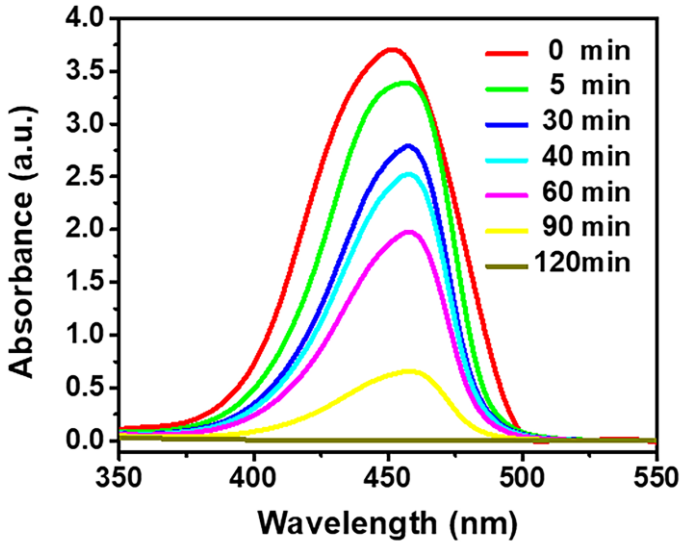

Figure S9. UV–Vis spectra for catalytic reduction of NN over Pd@MTP-3.

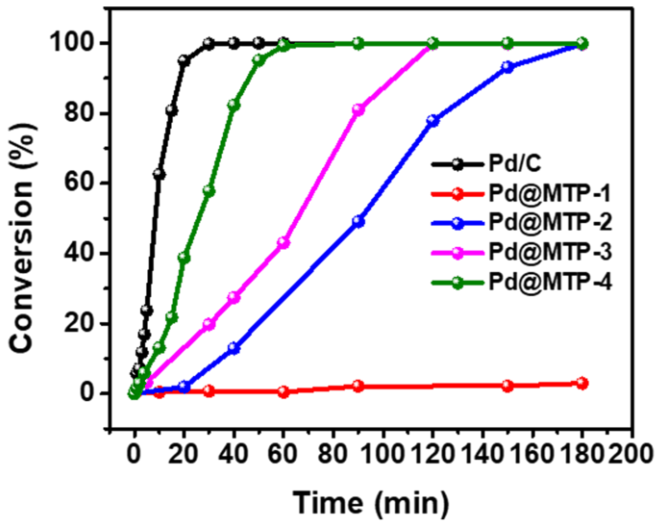

Figure S10. Conversion rates of Pd@MTP and Pd/C catalysts on catalytic reduction of NN.

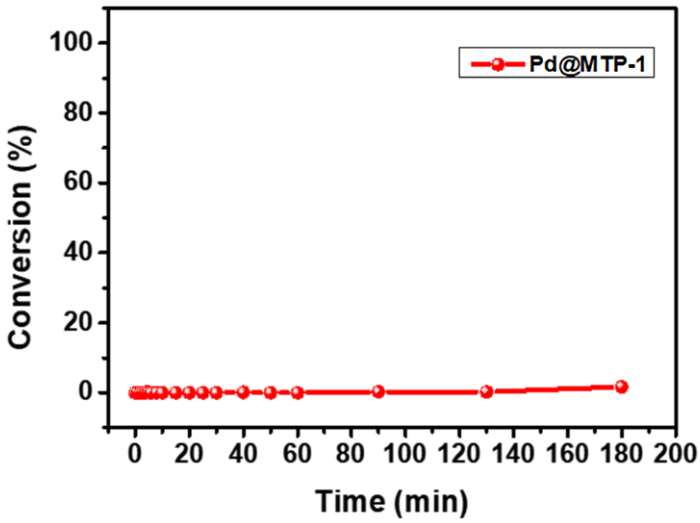

Figure S11. Conversion rates of Pd@MTP-1 on catalytic reduction of MG 17.

2. Supporting Tables

Table S1. Comparison of kinetic constant of catalytic *p*-NPh

Catalysts	Rate constant k (min^{-1})	Ref.
Pd embedded	0.0052	1
Pd@CHC	0.048	2
Pd@CH	0.033	2
Fe_xO_y/Pd@mSiO_2	0.096	3
CS/GA/RGO/Pd	0.0348	4
PEI-Pd0.5	0.080	5
CS/Pd-0.5%	0.117	6
Pd@MTP-3	0.070	This work

Table S2. Size-selectivity performance test of Pd@MTP-3 for Suzuki Coupling[a]

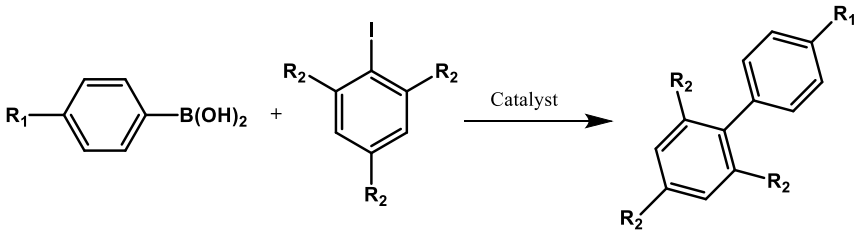

A **B**

entry	R1	R2	Catalyst	Yield (%)[b]
1	H	H	Pd@MTP-3	99
2	H	H	Pd/C	97
3	H	H	Pd@MTP-1	4
4	H	$-CH_3$	Pd@MTP-3	12
5	H	$-CH_3$	Pd/C	41
6	H	$-CH_3$	Pd@MTP-1	1
7	$-OCH_3$	H	Pd@MTP-3	74
8	$-OCH_3$	H	Pd/C	99
9	$-OCH_3$	H	Pd@MTP-1	3
10	$-OCH_3$	$-CH_3$	Pd@MTP-3	2
11	$-OCH_3$	$-CH_3$	Pd/C	55
12	$-OCH_3$	$-CH_3$	Pd@MTP-1	--

[a] Reaction conditions: A (1.1 mmol), B (1.0 mmol) , K_2CO_3 (1.5 mmol),catalyst (containing 0.2 mg Pd), DMF/H_2O (3mL/3mL), 60°C under nitrogen atmosphere. [b] determined by GC with hexadecane as internal standard.

Table S3. Catalytic Results from the Hydrogenation of Alkenes[a]

Catalyst	Substrate	Product	Conversion(%) [b]
Pd@MTP-3	hexene	hexane	98
Pd/C	hexene	hexane	99
Pd@MTP-1	hexene	hexane	--
Pd@MTP-3	cyclooctene	cyclooctane	35
Pd/C	cyclooctene	cyclooctane	56
Pd@MTP-1	cyclooctene	cyclooctane	--

[a] Reaction conditions: hexene (1mmol), cyclooctene (0.2 mmol). Pd@MTP-3 Catalyst (10mg), ethyl acetate (5 ml), 1bar H_2 room temperature. [b]determined by GC with decane as the internal standard.

3. Supported NMR data for prepared organic compounds

Biphenyl: ^{1}H NMR (500 MHz, $CDCl_3$) δ 7.62 (d, *J* = 7.9 Hz, 4H), 7.46 (t, *J* = 7.7 Hz, 4H), 7.37 (t, *J* = 7.4 Hz, 2H).^{13}C NMR (126 MHz, $CDCl_3$) δ= 141.37, 128.89, 127.35.

P-Methoxybiphenyl: ^{1}H NMR (500 MHz, $CDCl_3$) δ 7.59 – 7.52 (m, 4H), 7.43 (t, *J* = 7.7 Hz, 2H), 7.31 (t, *J* = 7.4 Hz, 1H), 6.99 (d, *J* = 8.8 Hz, 2H), 3.86 (s, 3H).^{13}C NMR (126 MHz, $CDCl_3$) δ= 159.27, 140.96, 133.91, 128.86, 128.29, 126.84, 114.33, 55.48.

2,4,6-Trimethylbiphenyl: ^{1}H NMR (500 MHz, $CDCl_3$) δ 7.43 (t, *J* = 7.5 Hz, 2H), 7.34 (t, *J* = 7.4 Hz, 1H), 7.16 (d, *J* = 6.9 Hz, 2H), 6.96 (s, 2H), 2.35 (s, 3H), 2.02 (s, 6H).^{13}C NMR (126 MHz, $CDCl_3$) δ=141.22, 139.20, 136.69, 136.11, 129.43, 128.49, 128.18, 126.63, 21.17, 20.88.

1,1'-Biphenyl, 4'-methoxy-2,4,6-trimethyl :^{1}H NMR (500 MHz, $CDCl_3$) δ 7.05 (d, *J* = 8.7 Hz, 2H), 6.97 – 6.93 (m, 4H), 3.86 (s, 3H), 2.33 (s, 3H), 2.01 (s, 6H).^{13}C NMR (126 MHz, $CDCl_3$) δ=158.33, 138.81, 136.56, 133.43, 130.45, 128.16, 113.90, 55.34, 20.93.

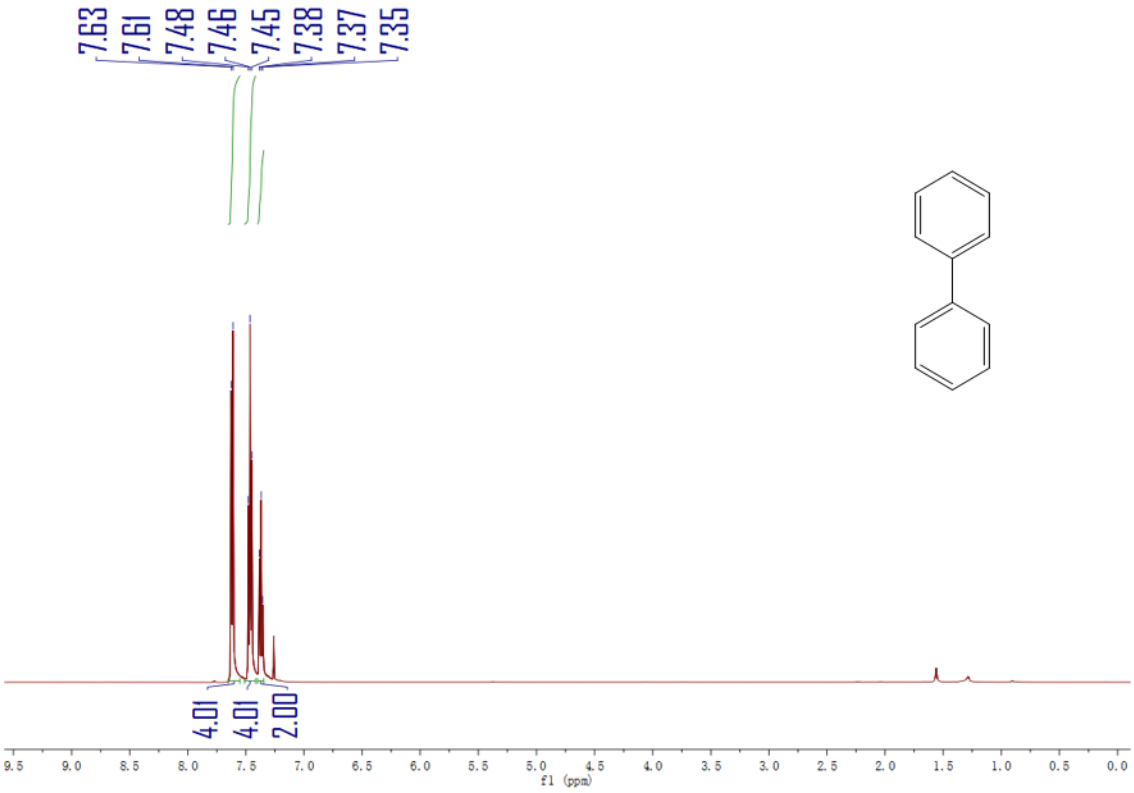
7.63
7.61
7.48
7.46
7.45
7.38
7.37
7.35
4.01
4.01
2.00
f1 (ppm)

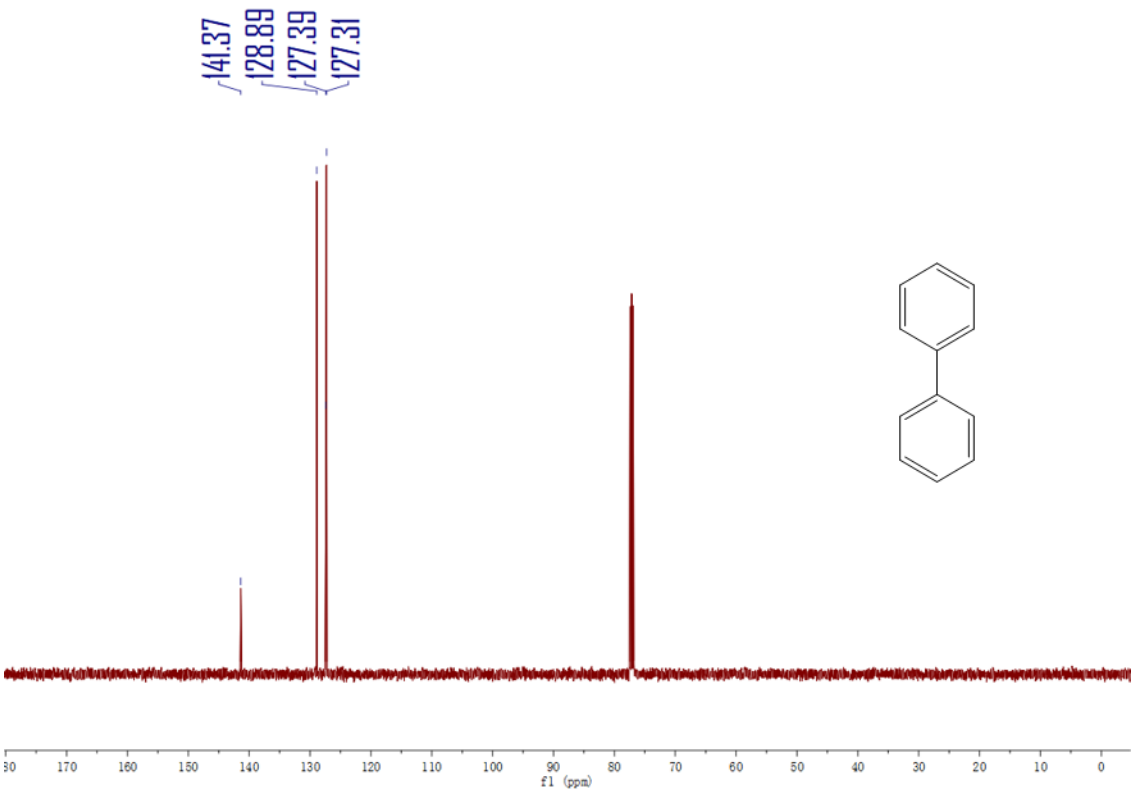
141.37
128.89
127.39
127.31
f1 (ppm)

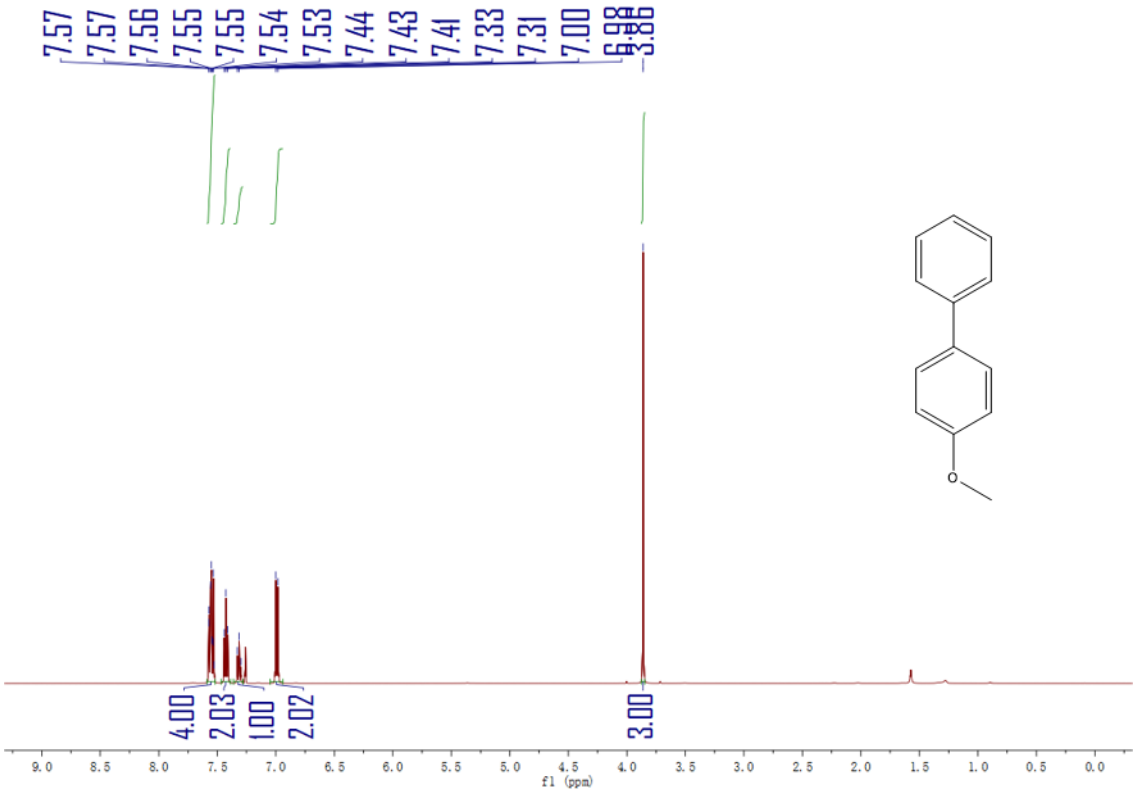
7.57
7.57
7.56
7.55
7.55
7.54
7.53
7.44
7.43
7.41
7.33
7.31
7.00
6.98
3.86
4.00
2.03
1.00
2.02
3.00
f1 (ppm)

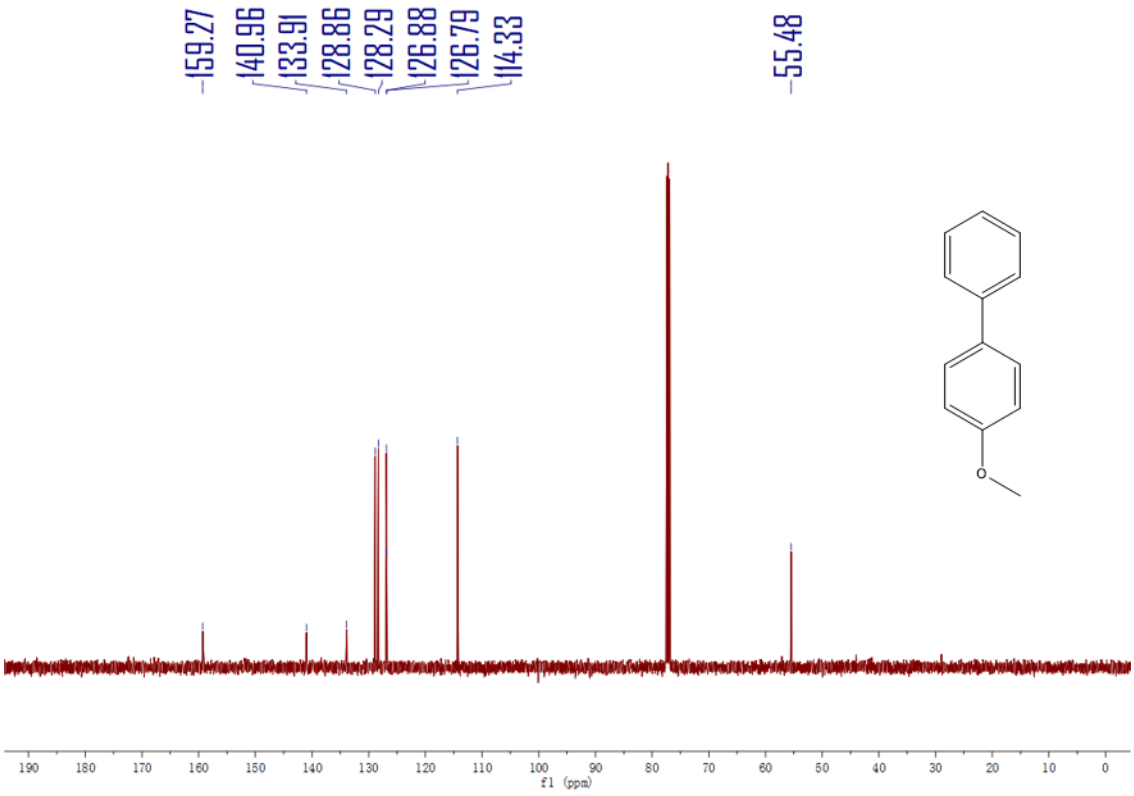
159.27
140.96
133.91
128.86
128.29
126.88
126.79
114.33
55.48
f1 (ppm)

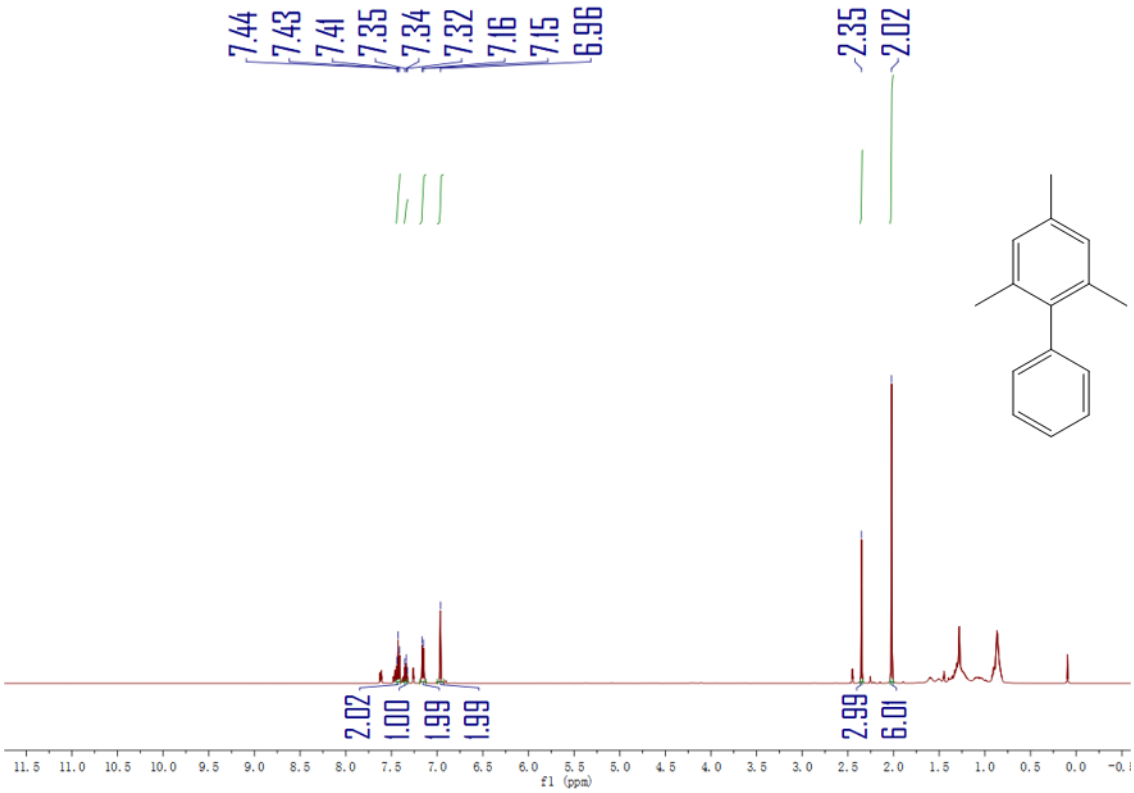
7.44
7.43
7.41
7.35
7.34
7.32
7.16
7.15
6.96
2.35
2.02
2.02
1.00
1.99
1.99
2.99
6.01
f1 (ppm)

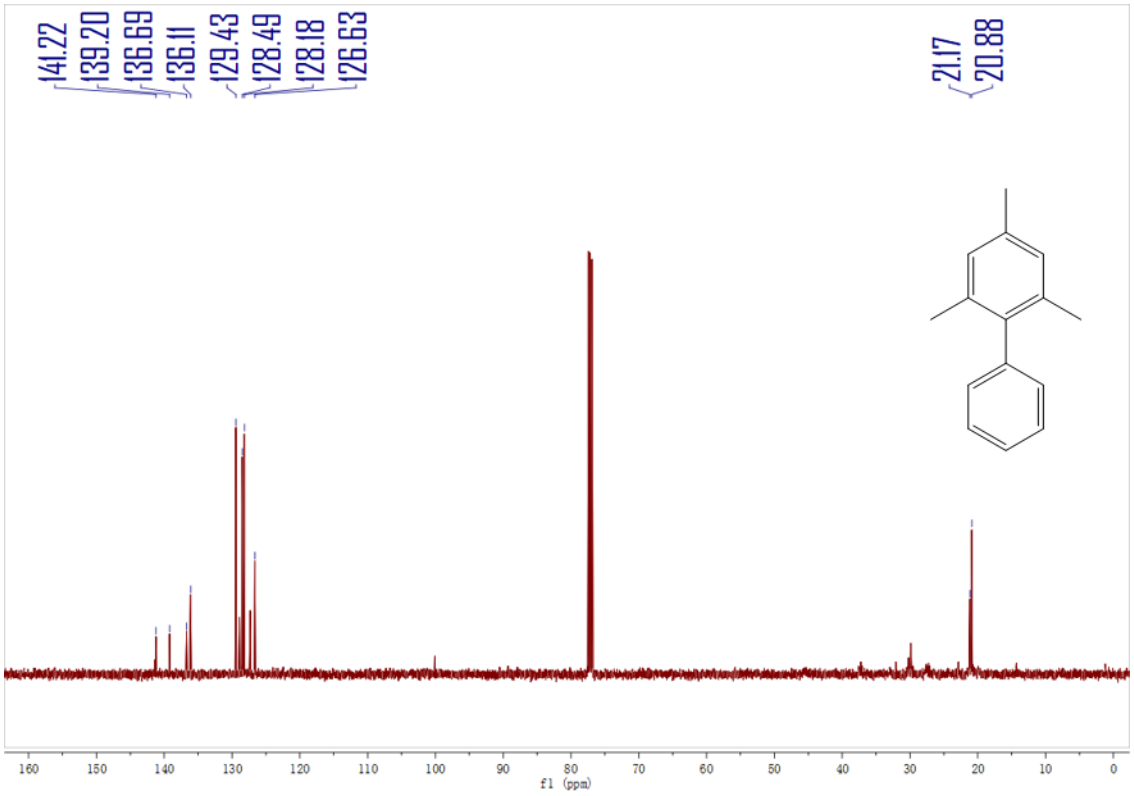
141.22
139.20
136.69
136.11
129.43
128.49
128.18
126.63
21.17
20.88
f1 (ppm)

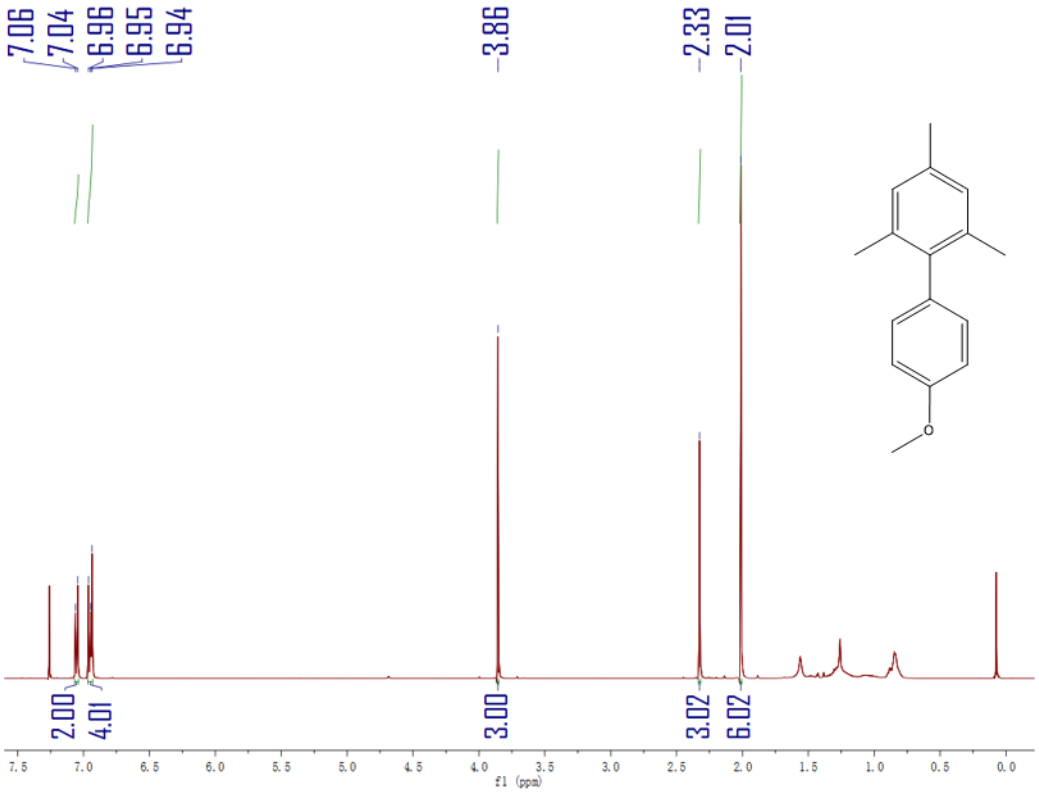
7.06
7.04
6.96
6.95
6.94
3.86
2.33
2.01
2.00
4.01
3.00
3.02
6.02
f1 (ppm)

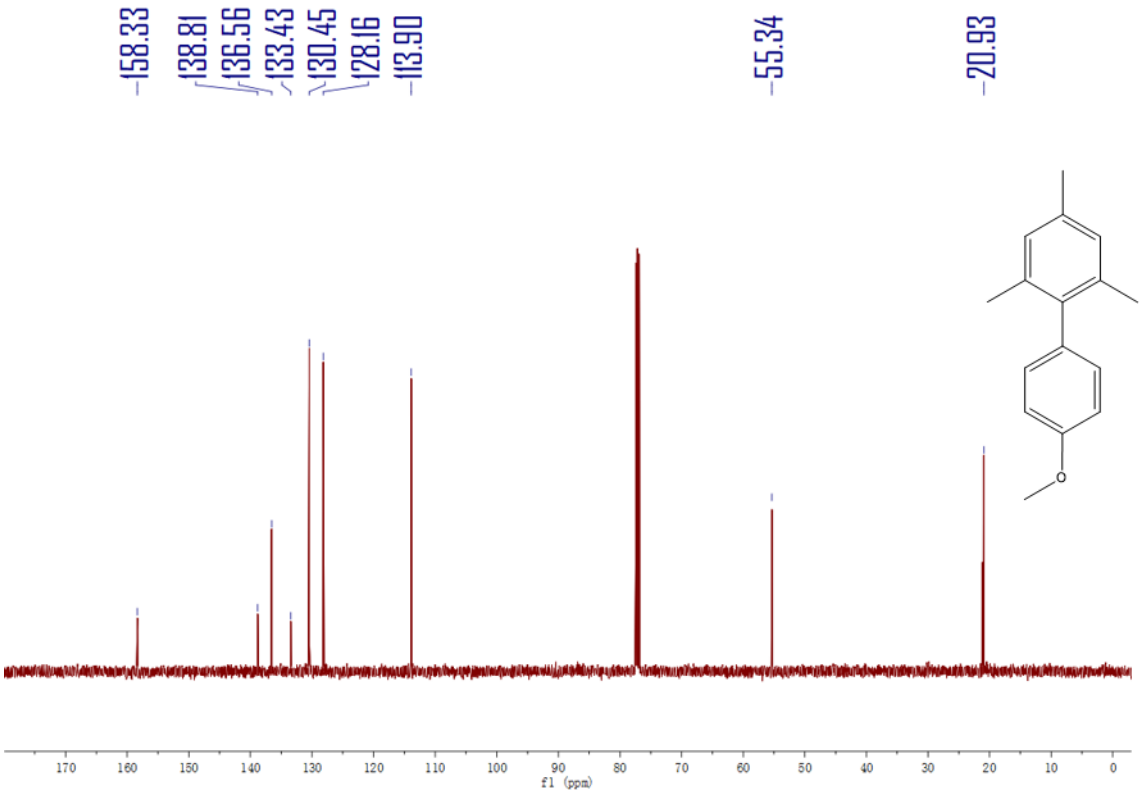
158.33
138.81
136.56
133.43
130.45
128.16
113.90
55.34
20.93
f1 (ppm)

Supplementary References:

[1] Xia, M.; Kang, S.-M.; Lee, G.-W.; Huh, Y. S.; Park, B. J. The recyclability of alginate hydrogel particles used as a palladium catalyst support. *J. Ind. Eng. Chem.* **2019**, *73*, 306-315.

[2] Li, X.; Dong, F.; Zhang, L.; Xu, Q.; Zhu, X.; Liang, S.; Hu, L.; Xie, H. Cellulosic protic ionic liquids hydrogel: A green and efficient catalyst carrier for Pd nanoparticles in reduction of 4-nitrophenol in water. *Chem. Eng. J.* **2019**, *372*, 516-525.

[3] Yao, T.; Cui, T.; Fang, X.; Cui, F.; Wu, J. Preparation of yolk–shell FexOy/Pd@mesoporous SiO2 composites with high stability and their application in catalytic reduction of 4-nitrophenol. *Nanoscale* **2013**, *5*, 5896-5904.

[4] Ge, L.; Zhang, M.; Wang, R.; Li, N.; Zhang, L.; Liu, S.; Jiao, T. Fabrication of CS/GA/RGO/Pd composite hydrogels for highly efficient catalytic reduction of organic pollutants. *RSC Adv.* **2020**, *10*, 15091-15097.

[5] Feng, Y.; Yin, J.; Liu, S.; Wang, Y.; Li, B.; Jiao, T. Facile Synthesis of Ag/Pd Nanoparticle-Loaded Poly(ethylene imine) Composite Hydrogels with Highly Efficient Catalytic Reduction of 4-Nitrophenol. *ACS Omega* **2020**, *5*, 3725-3733.

[6] Dhanavel, S.; Manivannan, N.; Mathivanan, N.; Gupta, V. K.; Narayanan, V.; Stephen, A. Preparation and characterization of cross-linked chitosan/palladium nanocomposites for catalytic and antibacterial activity. *J. Mol. Liq*. **2018**, *257*, 32-41.